Astron. Astrophys. 306, 436–442 (1996)

ASTRONOMY AND ASTROPHYSICS

Asteroseismology of the β Cephei stars

I. 16 (EN) Lacertae

W.A. Dziembowski[1] **and M. Jerzykiewicz**[2]

[1] Copernicus Astronomical Center, Polish Academy of Sciences, ul. Bartycka 18, PL-00-716 Warsaw, Poland
Internet: wd@camk.edu.pl
[2] Wroclaw University Observatory, ul. Kopernika 11, PL-51-622 Wroclaw, Poland
Internet: mjerz@astro.uni.wroc.pl

Received 5 April 1995 / Accepted 8 June 1995

Abstract. 16 (EN) Lacertae is a single-lined spectroscopic binary and an eclipsing variable. It consists of the well-known β Cephei star and an invisible secondary. Four pulsation modes, including a radial one, are found to be simultaneously present in the β Cephei primary.

We consider all possible identifications of the observed pulsation frequencies with the computed ones for low-degree modes ($l \leq 2$) in a series of stellar models covering the range of $T_{\rm eff}$ and mean density consistent with the best available data. Only models allowing no overshooting are taken into account and with this restriction the conclusion that the rotation rate increases inward is unavoidable. There are ambiguities in the identification of the modes. We recommend observations that should enable a unique identification and, as a result, yield precise model parameters and better constraints on the differential rotation.

Key words: stars: variable – stars: oscillations – stars: 16 Lac=EN Lac

1. Introduction

Significance of the β Cephei stars for asteroseismic probing of stellar interiors has been already emphasized in several papers. Dziembowski & Pamyatnykh (1993, henceforth DP) pointed out that these variables offer similar asteroseismic potential as do the δ Scuti stars. In both cases theory predicts opacity-driven modes which penetrate the whole interior. Prospects therefore exist for using the frequency data to address such unsolved problems of the stellar evolution theory as transport of angular momentum in the radiative interior or the extent of overshooting from the convective core.

Send offprint requests to: W.A. Dziembowski

The difficulties for both these types of stars are also similar. In individual objects, only a small fraction of the unstable modes is observed. For example, the ten modes detected by Breger et al. (1995) in FG Vir, the best case among the δ Scuti stars, constitute only about 10 percent of the $l \leq 2$ modes predicted to be unstable. Consequently, the observed frequency spectra are too sparse to exhibit patterns which would allow unambiguous mode identification. Other methods of observational identification of the spherical harmonic indices of the excited modes require high quality photometric and spectroscopic data which are not easy to obtain. Thus, the data available so far are insufficient to separate the problem of probing internal rotation from that of testing models of internal structure.

16 (EN) Lac is a single-lined spectroscopic binary (Lee 1910, Struve & Bobrovnikoff 1925) and an eclipsing variable with orbital period $P_{\rm orb} = 12\overset{\rm d}{.}09684$ (Jerzykiewicz 1980). The system consists of the well-known β Cephei variable and an invisible secondary.

Three circumstances make the β Cephei primary exceptionally attractive as a target for asteroseismology. First, frequencies of as many as four of its pulsation modes are precisely known from time-series observations. Second, multicolor photometry and radial-velocity data show that one of the four modes is radial and, of course, which of them it is. Third, the orbital and eclipse solutions yield a reliable value of the star's mean density.

As far as we know, the present work is the first attempt in asteroseismology of a β Cephei variable. It follows a similar effort made by Goupil et al. (1993) for GX Peg, a δ Scuti variable with five modes detected. We follow their work in limiting possible identifications to the modes with $l \leq 2$. This is partially justified by the rather large (about fivefold) increase of the amplitude reduction factor between $l = 2$ and 3. Furthermore, we also regard the internal rotation rate as the primary degree of freedom in our effort of fitting observed and model frequencies. However, unlike our predecessors we ignore convective overshooting because, in our opinion, there is no compelling observational or theoretical evidence for introducing it. In this

way we circumvent the difficulty mentioned in the second paragraph of this Introduction.

The next paper in this series we plan to devote to 12 (DD) Lac, one of the two β Cephei stars in which equidistant frequency triplets have been found. The other one, ν Eri, also merits attention. Another excellent candidate is V381 Car (HD 92024), a member of the galactic cluster NGC 3293 and an eclipsing binary.

In Sect. 2 of the present paper we discuss observational data for our analysis, that is, the frequencies of the four pulsation modes, the spherical harmonic degrees of the three largest-amplitude ones, and the star's mean density. In Sect. 3 we constrain the range of models to be considered and use results of the linear nonadiabatic pulsation calculations to confront model frequencies with the observed ones. Here we identify all low-degree pulsation modes ($l \leq 2$) that can correspond to the observed ones and examine their properties. In this section we also discuss uncertainties of the analysis and include recommendations for the observer. Finally, in Sect. 4 we summarize our conclusions.

2. Data

2.1. The frequencies

Using extensive *UBV* observations, carried out in the summer and autumn of 1965 at Lowell Observatory, Jerzykiewicz (1993) has shown that out-of-eclipse light variations of 16 Lac can be represented as a sum of nine sinusoidal terms. The three strongest terms, with frequencies $f_1 = 5.9112$ c/d, $f_2 = 5.8551$ c/d and $f_3 = 5.5033$ c/d, had been known before (Fitch 1969, Jerzykiewicz 1976). Frequencies of the six fainter ones are: $f_4 = 0.1653$ c/d, $f_5 = 7.194$ c/d, $f_6 = 11.822$ c/d, $f_7 = 11.358$ c/d, $f_8 = 11.414$ c/d and $f_9 = 11.766$ c/d. The first of these is equal to twice the orbital frequency. This suggests that the f_4 term may be caused by an "ellipticity effect." However, neither the amplitude nor the phase of the observed variation agree with such a possibility. The f_6 term is simply the lowest order harmonic of the f_1 term, and the three last ones are the first-order combination terms $f_2 + f_3$, $f_1 + f_3$ and $f_1 + f_2$.

The frequencies we will be concerned with in the present paper are the four frequencies f_1, f_2, f_3 and f_5. The latter may therefore be referred to as "the fourth frequency." In order to avoid confusion, we shall henceforth call it f_4 instead of f_5.

2.2. The l values

Stamford & Watson (1977) showed that in the case of the β Cephei stars, the *UBV* color-to-light amplitude ratios can be used to distinguish between the radial and quadrupole pulsation modes. An improved and extended version of this work has been subsequently published by Watson (1988). Using an analytic formula, originally derived by Dziembowski (1977), Watson (1988) expressed the light variation caused by a single pulsation mode, $\Delta m(l,t)$, as a sum of two cosine terms, $A_1 \cos 2\pi ft$ and $A_2 \cos(2\pi ft + \Psi_T)$, where f is the pulsation frequency, and Ψ_T is the phase shift between local effective temperature variation and local radius variation. A_1 and A_2 are functions of the spherical harmonic degree of the mode, l, the ratio of local fractional effective temperature amplitude to local fractional radius amplitude, $\mathscr{B}$, and parameters obtainable from model stellar atmospheres. Adopting stationary model atmospheres of Kurucz (1979), Watson (1988) was able to use the expression for $\Delta m(l,t)$ to obtain the color amplitude to visual amplitude ratio, A_{U-V}/A_V, and the color phase minus visual phase difference, $\Phi_{U-V} - \Phi_V$, as a function of l, Ψ_T, and $\mathscr{B}$. Since nonadiabatic eigenfunctions for models of the β Cephei stars were not available at the time, all Watson (1988) could do was to allow Ψ_T and $\mathscr{B}$ to vary within suitable limits in order to trace outlines of "areas of interest" in the $\Phi_{U-V} - \Phi_V$, A_{U-V}/A_V plane, that is, areas corresponding to a given l that can be occupied by β Cephei stars. In particular, he found that for $-5^o < \Phi_{U-V} - \Phi_V < 5^o$ one should expect $A_{U-V}/A_V > 0.45$ if $l = 0$, $0.35 < A_{U-V}/A_V < 0.45$ if $l = 1$, and $0.1 < A_{U-V}/A_V < 0.35$ if $l = 2$.

Amplitudes of the three strongest terms in the variation of EN Lac are known to vary on a time scale of years (Fitch 1969, Jerzykiewicz et al. 1984). Fortunately, in 1965, when observations mentioned in the preceding subsection were obtained, the *UBV* amplitudes of these terms exceeded 10 mmag. Since the mean errors amounted to 0.5 mmag in U and 0.15 mmag in V, the A_{U-V}/A_V ratios could be derived with good accuracy. The ratios turned out to be equal to 0.88 ± 0.03, 0.33 ± 0.05 and 0.42 ± 0.05 for f_1, f_2 and f_3, respectively. At the same time, the $\Phi_{U-V} - \Phi_V$ differences were all close to zero. Using these numbers and the above-mentioned Watson's (1988) inequalities, Jerzykiewicz (1993) concluded that the f_1 term should be identified with a radial mode, the f_2 term with an $l = 2$ mode, and the f_3 term with an $l = 1$ mode.

Finding only one radial mode among the three strongest terms is, of course, consistent with their close frequency spacing. Interestingly, the close f_1, f_2 doublet is not due to rotational splitting of two m states belonging to the same l, but consists of two modes of different l.

The f_4 term had its V amplitude equal to only 1.4 ± 0.15 mmag, and an undetectably low U amplitude, so that the A_{U-V}/A_V ratio could not be obtained. Deriving l for this mode by Watson's (1988) method must await much better data than those available at present.

Once nonadiabatic eigenfunctions for models of the β Cephei stars became available, the "areas of interest" in the $\Phi_{U-V} - \Phi_V$, A_{U-V}/A_V plane could be reduced to points with coordinates determined by the equilibrium parameters of the models. Using nonadiabatic eigenfunctions of DP, Cugier et al. (1994) constructed the color-to-light amplitude ratio *vs.* the phase difference diagrams for several photometric systems. For the U and V bands their results support those of Watson (1988). Cugier et al. (1994) considered also diagnostic properties of other diagrams, including the one with A_{U-V}/A_V as abscissa and the ratio of the radial-velocity amplitude, K, to A_V as ordinate. In this diagram $l = 0$, 1 and 2 are particularly well resolved.

According to Fitch (1969), the velocity-to-light amplitude ratios for the f_1, f_2 and f_3 terms amount to about 6.2, 3.0

and 2.0 km s^{-1} percent mean light, respectively. Since Fitch (1969) used B filter observations transformed to the intensity scale, his K to A_B ratios would be equal to 570, 280 and 184 km s^{-1}/mag. These numbers are smaller than 706 ± 29, 443 ± 52 and 479 ± 31 km s^{-1}/mag, the K/A_b ratios we derived from the radial-velocity observations of Le Contel et al. (1983) and the Strömgren b photometry of Jerzykiewicz et al. (1984). Taking into account the color-to-magnitude ratios A_{B-V}/A_B, which are equal to 0.10, 0.04, and 0.06 (Jerzykiewicz 1993), we get K/A_V equal to 640, 310 and 190 km s^{-1}/mag if we use Fitch's (1969) numbers, and 789 ± 32, 492 ± 58 and 499 ± 32 km s^{-1}/mag, if we use ours. Plotted in the K/A_V *vs.* A_{U-V}/A_V diagram of Cugier et al. (1994), both K/A_V values for the f_1 term indicate an $l = 0$ mode. On the other hand, Fitch's (1969) K/A_V ratios for f_2 and f_3 can only be reconciled with $l = 2$, while ours, with $l = 1$.

These results should be compared with those based on Watson's (1988) method. For f_1 both methods agree. There is thus no doubt that this mode is radial. For f_2 the color-to-light amplitude ratio identification is consistent with the velocity-to-light amplitude ratio of Fitch (1969), while for f_3, with ours. However, adding one standard deviation to the f_2 value of A_{U-V}/A_V would shift it into the $l = 1$ area. Clearly, deciding between an $l = 1$ and $l = 2$ mode is impossible in this case. On the other hand, over two standard deviations would have to be subtracted from the A_{U-V}/A_V value for f_3 in order to shift it into the $l = 2$ area. Moreover, in the data used by Fitch (1969) the amplitude of this term was very small and variable, so that his velocity-to-light amplitude ratio must be rather uncertain. Giving lower weight to Fitch's (1969) K/A_V value we therefore conclude that in the case of f_3 the $l = 1$ identification is more probable than the $l = 2$ one.

2.3. The mean density

Pigulski & Jerzykiewicz (1988) have noticed that combining the photometric and spectroscopic elements of 16 Lac leads to a mass-radius relation which yields very nearly the same mean density for a range of mass of the primary. Indeed, for $7\ M_\odot < M < 15\ M_\odot$, where M is the primary's mass, the mean density can be represented by the interpolation formula

$$\langle\rho\rangle = 0.0356\, M^{0.042}, \qquad (1)$$

where $\langle\rho\rangle$ is expressed in solar units. The mean error of $\langle\rho\rangle$, resulting from the mean errors of the photometric and spectroscopic elements, is equal to $0.0053\ \langle\rho\rangle_\odot$.

3. Identification of pulsation modes

3.1. Models and the radial order of the f_1 mode

The models were constructed with the same code as that used in DP. This is a standard stellar evolution code allowing no effects of rotation and no convective overshooting. As a standard we adopted the OP opacity data (Seaton et al. 1994) and the element abundance parameters $X = 0.7$ and $Z = 0.02$. In Sect. 3.4 we shall also present sample results obtained with the OPAL opacities (Iglesias et al. 1992) and with different choices for X and Z.

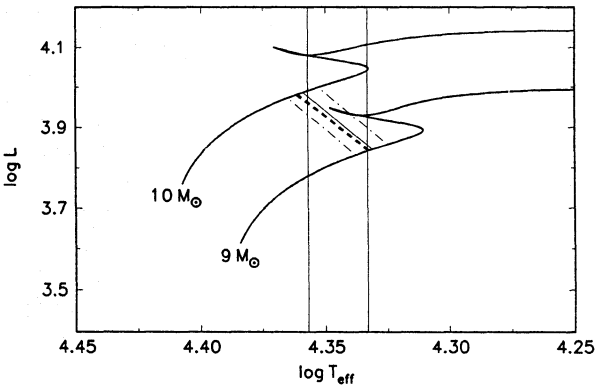

Fig. 1. The $\langle\rho\rangle$ = const and f = const lines and evolutionary tracks in the theoretical H-R diagram. Shown are the lines $\langle\rho\rangle = 0.0391\ \langle\rho\rangle_\odot$ (inclined thin solid line), $\langle\rho\rangle = 0.0391 \pm 0.0053\ \langle\rho\rangle_\odot$ (dash-dotted lines), and $f = f_1$ (thick dashed line). The tracks were computed for $X = 0.7$ and $Z = 0.02$ by means of the stellar evolution code mentioned in the text. The vertical lines represent the two values of the effective temperature of 16 Lac discussed in Sect. 3.1

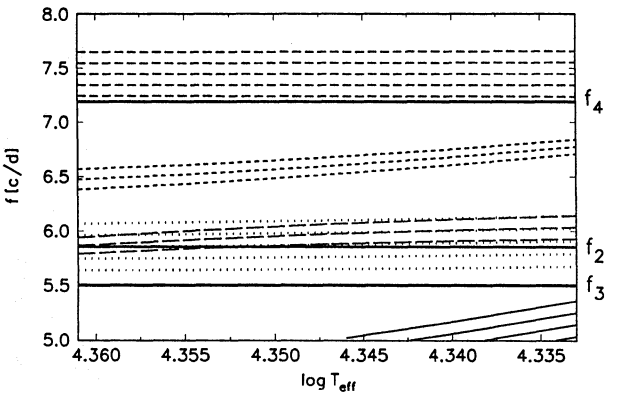

Fig. 2. Frequencies of modes with $l = 1$ (short- and long-dashed lines) and $l = 2$ (medium-dashed, dotted and thin-solid lines) for models in the 9 to 10 $M_\odot$ mass range plotted as a function of effective temperature. The rotational frequency splitting was calculated assuming $V_{\rm rot} = 40$ km s^{-1}. The three horizontal solid lines represent the observed frequencies f_2, f_3, and f_4. The model parameters were interpolated so that the fundamental radial mode frequency is exactly equal to the observed one, $f_1 = 5.9112$ c/d. There are no other $l \leq 2$ modes in the frequency range considered

Oscillation frequencies for the models were obtained in the same way as in DP, that is, by means of a fully nonadiabatic code which yields reliable growth rates. The code does not include the effects of rotation, but it returns the Ledoux constant which allows calculation of the rotational frequency splitting.

Given an observed value of the effective temperature and computed evolutionary tracks, the mass-radius relation can be used to plot the star in the theoretical H-R diagram. An example is shown in Fig. 1. The vertical lines mark two values

of $\log T_{\rm eff}$ of 16 Lac, equal to 4.357 and 4.333, both derived from the Strömgren indices. The higher value was obtained by Jerzykiewicz & Sterken (1980), while the lower one by Shobbrook (1985). Since the same photometric data and dereddening procedure were used in both cases, the difference in $\log T_{\rm eff}$ reflects a difference in the temperature calibrations of the indices. The mass-radius relation is the inclined solid line that crosses the 10 and 9 $M_\odot$ tracks close to where they intersect the two vertical lines. Thus, the two photometric values of $\log T_{\rm eff}$ define a mass range from 10 to 9 $M_\odot$. However, the correct value of the mass is probably close to the upper bound of this range because the higher value of $\log T_{\rm eff}$ is more nearly consistent with the most recent temperature calibrations of the Strömgren indices, provided by Napiwotzki et al. (1993) and Balona (1994). Indeed, using these calibrations and the same photometric data as before one gets $\log T_{\rm eff}$ equal to 4.358 and 4.351, respectively.

From Eq. (1) it follows that $\langle\rho\rangle = 0.0392\ \langle\rho\rangle_\odot$ for $M = 10\ M_\odot$, and $0.0390\ \langle\rho\rangle_\odot$ for $9\ M_\odot$. Thus, the mass-radius line in Fig. 1 is in fact a $\langle\rho\rangle$ = const line. The two dash-dotted lines in this figure represent the lower and upper bounds of $\langle\rho\rangle$, determined by the above-mentioned mean error of $0.0053\ \langle\rho\rangle_\odot$. The band so defined cuts the evolutionary tracks at the advanced stages of core-hydrogen burning.

Computed frequencies of the radial fundamental mode for core-hydrogen burning models along the $\langle\rho\rangle$ = const line in Fig. 1 turn out to be close to the observed frequencies f_1, f_2, and f_3. Therefore, the f_1 mode, which was shown in Sect. 2.2 to be radial, must be the radial fundamental mode.

3.2. One-dimensional family of stellar models

The observed value of $\langle\rho\rangle$, although crucial in identifying the radial order of the f_1 mode, is of no further use because of its relatively large mean error. On the other hand, the frequencies are practically error-free. We shall therefore rely on them in the following discussion.

First of all, we shall require that the computed frequency of the radial fundamental mode should be exactly equal to f_1. This condition selects a one-dimensional family of stellar models to be used in the next two sections for considering plausible identifications for the three remaining modes. In the H-R diagram, the models define an f = const line (the thick dashed line in Fig. 1), almost coinciding with the $\langle\rho\rangle = 0.0391\ \langle\rho_\odot\rangle$ line. The two lines are very nearly parallel because *the pulsation constant* is indeed very nearly constant for the set of models considered here. We shall treat the whole 9 to 10 $M_\odot$ range as the allowed range for the mass of EN Lac, although – as the $f = f_1$ line in Fig. 1 shows – the upper mass limit consistent with the upper limit of $T_{\rm eff}$ is somewhat lower. The range of the star age corresponding to this mass range is 20 to 16 million years and that of the H abundance in the core is 0.196 to 0.231.

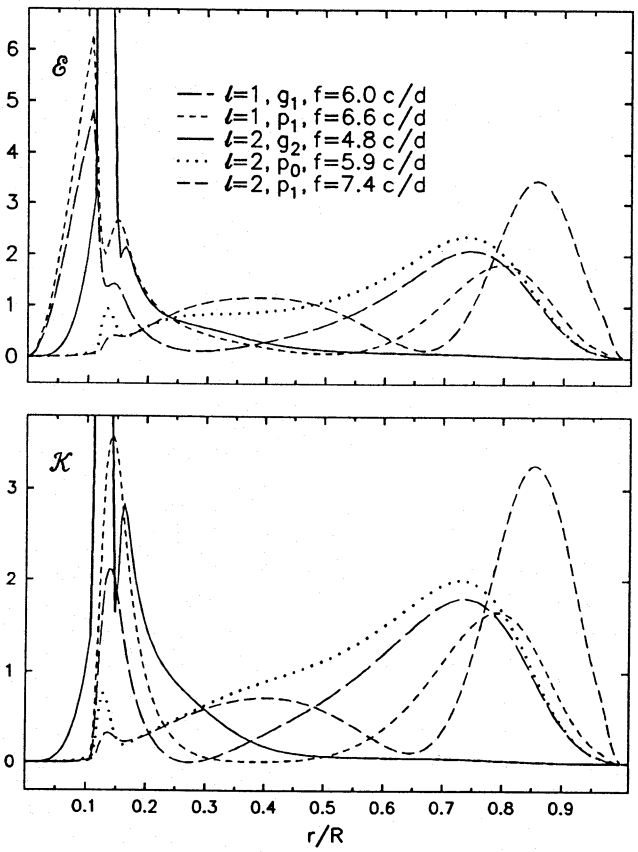

Fig. 3. Differential distribution of kinetic energy $\mathscr{E}$ (upper panel) and the rotational splitting kernel $\mathscr{K}$ (lower panel) plotted as a function of fractional radius in the model with $M = 9.5\ M_\odot$ and $\log T_{\rm eff} = 4.346$ for selected modes. The line coding is the same as in Fig. 2. For the g_2, $l = 2$, $f = 4.8$ c/d mode (solid lines), the maxima of $\mathscr{E}$ and $\mathscr{K}$ at $r = 0.13R$ are 34 and 28, respectively.

3.3. Nonradial modes

Fig. 2 shows how frequencies of nonradial modes vary within the one-dimensional family of models defined in the preceding subsection. The rotational splitting was calculated assuming the usual linear formula, valid for slow and uniform rotation:

$$f_m = f_0 + m\frac{V_{\rm rot}}{2\pi R}(1 - C), \qquad (2)$$

where m is the azimuthal order, $V_{\rm rot}$ is the equatorial velocity of rotation, and C is the Ledoux constant. We adopted $V_{\rm rot} = 40$ km s^{-1}. This number is equal to a mean of two $V_{\rm rot} \sin i$ values from the literature, 37 km s^{-1} (Lesh & Aizenman 1978) and 23 km s^{-1} (Hoffleit 1982), divided by $\langle \sin i\rangle$. Note, however, that the choice of $V_{\rm rot}$ is not essential in our discussion since it is the r-dependent rotation frequency, $f_{\rm rot}(r)$, which we shall regard as the primary adjustable quantity (see below).

There are striking differences in the frequency behavior between the five multiplets shown in the figure. In the two higher frequency $l = 2$ multiplets, the frequencies are very nearly constant, while in the $l = 1$ multiplets and the low frequency $l = 2$ multiplet the frequencies increase with decreasing $T_{\rm eff}$. Further-

more, in the case of the higher frequency $l = 1$ multiplet there is a visible decrease in the rotational splitting with decreasing $T_{\rm eff}$.

The differences in the frequency behavior are connected with differences in the physical nature of the considered modes. In order to show this we plotted in Fig. 3 the normalized distribution of the mode kinetic energy $\mathscr{E}$ (upper panel) and the rotational kernel $\mathscr{K}$ (lower panel). The latter allows calculating the rotational splitting in the case of the r-dependent rotation frequency, $f_{\rm rot}(r)$, according to the following expression:

$$f_m - f_0 = \int \mathscr{K} f_{\rm rot}(r) d\frac{r}{R}. \qquad (3)$$

As can be seen from Fig. 3, the $l = 2$, $f \approx 7.4$ c/d mode has its energy concentrated in the outer part of the envelope where the acoustic propagation zone occurs. Thus, it may be regarded as a p mode, although the maxima of $\mathscr{E}$ and $\mathscr{K}$ at $r \approx 0.13R$ within the gravity propagation zone tell us that the mode is mixed. The frequency of this mode, like frequencies of the radial modes, is determined by the acoustic properties of the envelope. Therefore, it is not surprising that this frequency is nearly constant in the sequence of models with fixed radial p_1-mode frequency.

The amplitude of the $l = 1$, $f \approx 6.6$ c/d mode has a pronounced maximum at $r \approx 0.1R$, exactly at the edge of the convective core. This mode is peculiar because it has relatively large oscillation amplitude in the convective core. A more typical g mode such as the $l = 2$, $f \approx 4.8$ c/d one has its energy strongly confined in the chemically inhomogeneous zone between $r/R = 0.1$ and 0.15, that is, between the current edge of the core and that in the ZAMS model.

The two $l = 1$ modes have so close frequencies and so similar shapes of $\mathscr{E}$ and $\mathscr{K}$ because we are not far from the avoided crossing between p_1 and g_1. Let us observe the behavior of the rotational frequency splitting in Fig. 2. At the high $T_{\rm eff}$ end the splitting is bigger for the higher-frequency mode but with the decrease of $T_{\rm eff}$ the situation gradually reverses. This trend reflects the shift in the relative contribution to $\mathscr{K}$ from the two propagation zones. (Let us remind the reader that for the g modes $C \approx 1/l(l+1)$ while for the p modes $C \ll 1$, and that the rotational splitting $\propto 1 - C$.) One should also note the difference in behavior, as well as in amplitude, between $\mathscr{E}$ and $\mathscr{K}$ for the $l = 1$ modes.

Before proceeding with the identification of the frequencies f_2, f_3, and f_4, we need to define the radial order of the multiplets. The dual nature of the considered modes causes an ambiguity. Here we adopt the following nomenclature. In the $l = 1$ sequence, the mode of the lower frequency we name g_1, and that of the higher frequency, p_1. Note, however, that at the low mass end the former is in fact a p mode rather than a g mode. In the $l = 2$ sequence, the consecutive multiplets we name g_2, p_0, and p_1.

As can be seen from Fig. 2, f_2 may be identified with the $m = 0$ modes whose frequencies are independent of the rotation as long as the second order effects of rotation are ignored. There are two such possibilities. One is $l = 2$, p_0. This implies $\log T_{\rm eff} = 4.358$ and $M = 9.9\ M_\odot$. The other possibility is $l = 1$, g_1, formally implying a mass somewhat above the allowed upper limit of $10\ M_\odot$. Nevertheless, in view of uncertainties, we regard this identification as tenable. Discrimination between these two $m = 0$ modes should be possible with precise measurements of the light and color phases for the f_2 term. Closer to the lower mass limit, the $l = 1$, $m = -1$, g_1 is also a possibility. More accurate values of $T_{\rm eff}$ would help discriminate between this and the two previous options.

A support for a mass closer to the upper limit comes from considerations of the conditions for mode driving. In none of the models calculated with the use of the OP opacities is it possible to excite a mode with frequency as high as f_4. At $M = 10\ M_\odot$ the modes with such frequencies are very close to instability, so that a slight enhancement of the Fe abundance would render them unstable. With the OPAL opacities we find instability in some range below $10\ M_\odot$, but at $M = 9\ M_\odot$ these modes are definitely stable. Modes with frequencies below 6 c/d were found unstable in all considered models.

Neither f_3 nor f_4 may be identified with any of the centroid frequencies in our models. A conservative identification of f_4 is $l = 2$, $m = -2$, p_1. This identification requires that the mean value of $f_{\rm rot}$ is larger than that assumed in the calculated rotational splitting. The required increase ranges from 21% for the $9\ M_\odot$ model to 24% for $10\ M_\odot$ model. The discrepancy may be due to an underestimate of $V_{\rm rot}$ or to an inward increase of $f_{\rm rot}$. The latter interpretation is supported by the possible identifications of f_3 which we are going to consider presently.

As we found in Sect. 2.2, an $l = 1$ identification is preferred for f_3 over an $l = 2$ one. Of the two $l = 1$ multiplets seen in Fig. 2, g_1 is much closer to f_3 than p_1, but it still implies a large increase of $f_{\rm rot}$ over the assumed value. The $l = 1$, $m = -1$, g_1 identification requires that the weighted mean value of $f_{\rm rot}$ should be increased from 380 to 400% over the range from 10 to $9\ M_\odot$, respectively. We can see from Fig. 3 that the kernels, $\mathscr{K}$, for the $l = 1$ modes sample two separate regions. One is the g-mode propagation zone at $r/R \approx 0.15$. The other is the p-mode propagation zone around $r/R \approx 0.7$. The relative contribution to the rotational splitting varies across the considered range of models. In the case of g_1 the largest contribution from the inner zone occurs at high mass end, while the opposite is true in the case of p_1. Let us note that the $l = 2, p_1$-mode kernel is very small in the inner zone and therefore it is possible that this mode will experience much lower frequency splitting if the rotation rate in this inner zone is much faster than in the envelope. In order to explain the difference in the splitting, we need to postulate that in the inner zone $f_{\rm rot}$ is larger than in the envelope by a factor of at least 8 to 10.

The computed frequency closest to f_3 is that of the $l = 2$, $m = -2$, p_0 mode. Although, according to Sect. 2.2, this option is less probable than the $l = 1$ one, it nevertheless remains possible. With this identification, the increase of $f_{\rm rot}$ needed to match the observed frequency ranges from about 61% of the adopted value at $10\ M_\odot$ to 73% at $9\ M_\odot$. As can be seen from Fig. 3, the main difference in the kernels for the $l = 2$ p_0 and p_1 modes occurs in the $r/R = 0.5$–0.7 range. An inward increase

in $f_{\rm rot}$ by a factor of $\sim$ 3 between r/R = 1 and 0.5 would account for the difference in the splitting of the p_0 and p_1 modes. However, this rise of $f_{\rm rot}$ in the chemically homogeneous zone may be difficult to accept because it causes instabilities which could only be prevented by a concentration gradient. Such a gradient exists in the narrow zone between $r/R = 0.1$ and 0.15, but the difference of the integrated kernels in this zone is only 0.01. Thus, to explain the difference in the splitting we would have to assume that in this narrow zone the mean value of $f_{\rm rot}$ is $\sim$ 100 times greater than in the outer layers. This is more than for the $l = 1$, $m = -1$, g_1 identification.

Another possible identification for f_3 is $l = 2$, $m = 2$, g_2. This mode, as it may be seen in Fig. 3, has its kernel almost entirely confined to the chemically inhomogeneous zone. At $M = 9\ M_\odot$ this identification requires a 63% increase of $f_{\rm rot}$ over the adopted value. The required increase growth rapidly with mass and, for instance, at $M = 9.5\ M_\odot$ it reaches 224%. Let us point out that we could discriminate between the two $l = 2$ identifications of f_3 if we knew the sign of m. In principle, the sign of m can be determined observationally by means of an analysis of the line-profile variations. In practice, however, the method may give inconclusive results. The recent attempt undertaken by Mathias et al. (1994) for 12 (DD) Lac can serve as an example of these difficulties. Nonetheless, in view of the far reaching implications of the expected result we strongly encourage such efforts. An important by-product of the work would be a better value of $V_{\rm rot} \sin i$ than the one available at present.

3.4. Uncertainties

There are uncertainties in our models. They concern chemical composition, effects of rotation, and convective overshooting. Fig. 4 shows how changes of X and Z affect $T_{\rm eff}$ and the frequencies of the four higher-frequency nonradial modes discussed in the preceding subsection. The effect of decreasing Z or X is similar to the effect of increasing mass. Since spectroscopic determination of the He/H abundance ratio is difficult, we must regard an asteroseismic mass determination based on a frequency measurement for one nonradial mode with $m = 0$ as uncertain. A crude estimate from Fig. 4 is

$$\Delta M/M \approx -1.2\Delta X/X. \qquad (4)$$

However, the effect of changing X cannot be exactly compensated for by a change of M for all modes simultaneously. This means that by measuring frequencies for two nonradial modes with $m = 0$ we could in principle determine both M and X.

We see from Fig. 4 that the frequency of the $l = 2, p_1$ mode is essentially unaffected by all these changes, which is of course the consequence of the predominantly acoustic nature of this mode and the fact that our models were selected to have the same frequency of the $l = 0$, p_1 mode. The figure shows also the encouraging fact that for all frequencies the effect of using the OPAL instead of the OP opacities is small.

We calculated our models assuming zero overshooting, but we should stress that this is not a generally accepted option. Convective overshooting has little effect on the p-mode frequencies

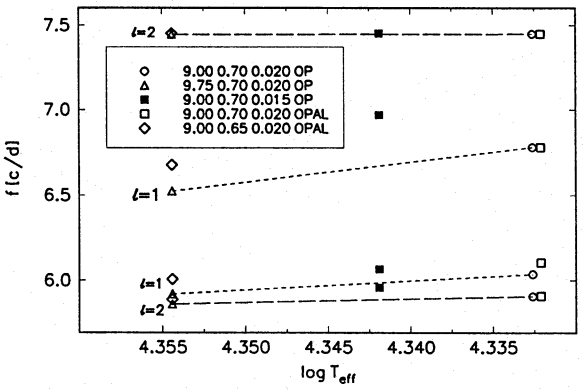

Fig. 4. Effects of changing opacity data (OPAL *vs.* OP) and composition parameters X and Z on the frequencies of the four higher-frequency nonradial modes discussed in Sect. 3.3. The effect of changing the mass from 9.00 to 9.75 $M_\odot$ is shown for comparison

but leads to significant decrease of the g-mode frequencies. Let us note that allowing for overshooting we could fit the $l = 1$, g_1-mode frequency to f_3 without invoking rapidly rotating interior. As long as we do not know the m value, both options remain viable. If, however, future line-profile observations should yield $m = 0$ for f_3, overshooting would remain the only possibility. In this case we could even calibrate the distance of overshooting.

Large values of $f_{\rm rot}$ in the deep interior suggested by our mode identifications may imply the need of taking into account centrifugal force in the models. Again, the g-mode frequencies will be primarily affected by such a modification.

4. Summary

The color-to-light and velocity-to-light amplitude ratios show that the f_1 mode is radial. The mean density of the star, amounting to $\langle\rho\rangle = 0.0391 \pm 0.0053\ \langle\rho\rangle_\odot$, implies then that this mode must be the fundamental, that is, p_1. As far as f_2 and f_3 are concerned, the amplitude ratios indicate $l = 1$ or 2. In the case of f_3 the first possibility is somewhat more probable than the second.

The observed value of the fundamental mode frequency determines a one-dimensional family of stellar models. We use models of normal Population I composition, $X = 0.7$ and $Z = 0.02$. The models span a mass range from 9 to 10 $M_\odot$, consistent with the range of the $\log T_{\rm eff}$ of 16 Lac obtained from the Strömgren indices. The range of the star age corresponding to this mass range is 20 to 16 million years, and that of the H abundance in the core is 0.196 to 0.231.

Considering possible identifications of the f_2, f_3 and f_4 modes we limited ourselves to spherical harmonic degrees $l \leq 2$. We found that f_2 can be identified with the $m = 0$ modes whose frequencies are independent of the rotation as long as the second order effects of rotation are ignored. There are two such modes in our models. One is $l = 2$, p_0. It yields the following parameters: $\log T_{\rm eff} = 4.358$ and $M = 9.9\ M_\odot$. The other is $l = 1, g_1$, formally implying a mass somewhat above the allowed

upper limit of 10 $M_\odot$. Closer to the lower mass limit, the $l = 1$, $m = -1$, g_1 mode is also a possibility.

Neither f_3 nor f_4 may be identified with any of the $m = 0$ modes. A conservative identification of f_4 is $l = 2$, $m = -2$, p_1. It requires the mean value of $f_{\rm rot}$ to be higher than that assumed in the calculated rotational splitting. The discrepancy may be due to an underestimate of the surface rotation velocity or to an inward increase of $f_{\rm rot}$.

The three possible identifications of f_3 are: (1) $l = 1$, $m = -1$, g_1, (2) $l = 2$, $m = -2$, p_0, and (3) $l = 2$, $m = 2$, g_2. As in the case of f_4, they all require that the mean value of $f_{\rm rot}$ should be increased over the assumed one. Consideration of the rotational splitting kernels then shows that in all three cases this implies significant inward increases of the rotation rate. Thus, regardless of which identification is correct, the conclusion that the interior of EN Lac rotates significantly faster than the outer layers is unavoidable.

Acknowledgements. This research was supported by KBN grants Nr 2 P304 013 07 and Nr 2 P304 001 04.

References

Balona, L. A. 1994, MNRAS, 268, 119
Breger, M., Handler, G., Nather, R. E., Wing et, D. E., Klansman, S. J., Scullion, D. J., Hi-ping, L., Sophism, J. E., Hi-yang, J., Long-li, L., Wood, M. A., Watson, T. K., Dziembowski, W. A., Serkowitsch, E., Mendelian, H., Clemens, J. C., Krzesinski, J., Pajdosz, G. 1995, A&A, 297, 473
Cugier, H., Dziembowski, W. A., Pamyatnykh, A. A. 1994, A&A, 291, 143
Dziembowski, W. 1977, Acta Astron., 27, 203
Dziembowski, W., Pamyatnykh, A. A. 1993, MNRAS, 262, 204
Fitch, W. S. 1969, ApJ, 158, 269
Goupil, M. J., Michael, E., Libretto, Y., Baling, A. 1993, A&A, 268, 546
Hoffleit, D. 1982, The Bright Star Catalogue, Yale University Observatory, New Haven, Connecticut, U. S. A.
Iglesias, C. A., Rogers, F. J., Wilson, B. G. 1992, ApJ, 397, 717
Jerzykiewicz, M. 1976, in Multiple Periodic Variable Stars, ed. by W. S. Fitch (Budapest: Akadémiai Kiadó), vol. 2, p. 39
Jerzykiewicz, M. 1980, in Nonradial and Nonlinear Stellar Pulsation, ed. by H. A. Hill & W. A. Dziembowski (Springer: Berlin, Heidelberg, New York), p. 125
Jerzykiewicz, M. 1993, Acta Astron., 43, 13
Jerzykiewicz, M., Sterken, C. 1980, in Variability in Stars and Galaxies, ed. by P. Ledoux (Institut d'Astrophysique, Liège), p. B.4.1
Jerzykiewicz, M., Borkowski, K. J., Musielok, B. 1984, Acta Astron., 34, 21
Kurucz, R. L. 1979, ApJS, 40, 1
Le Contel, J.-M., Ducatel, D., Jarzebowski, T., Jerzykiewicz, M., Valtier, J.-C. 1983, A&A, 118, 294
Lee, O. J. 1910, ApJ, 32, 307
Lesh, J. R., Aizenman, M. L. 1978, ARA&A, 16, 215
Mathias, P., Aerts, C., Gillet, D., Waelkens, C. 1994, A&A, 289, 875
Napiwotzki, R., Schönberner, D., Wenske, V. 1993, A&A, 268, 653
Pigulski, A., Jerzykiewicz, M. 1988, Acta Astron., 38, 401
Seaton, M. J., Yan, Y., Mihalas, D., Pradhan, A. K. 1994, MNRAS, 266, 805
Shobbrook, R. R. 1985, MNRAS, 214, 33
Stamford, P. A., Watson, R. D. 1977, MNRAS, 180, 551
Struve, O., Bobrovnikoff, N. T. 1925, ApJ, 62, 139
Watson, R. D. 1988, Ap&SS, 140, 255

This article was processed by the author using Springer-Verlag LaTeX A&A style file version 3.